



# Value of $^{18}\text{F}$ -FDG PET/CT in the diagnosis of portal vein tumor thrombus in patients with hepatocellular carcinoma

Bing Wu<sup>1,2,3</sup> · Yiqiu Zhang<sup>1,2,3</sup> · Hui Tan<sup>1,2,3</sup> · Hongcheng Shi<sup>1,2,3</sup> 

Published online: 3 April 2019  
© Springer Science+Business Media, LLC, part of Springer Nature 2019

## Abstract

**Objective** The aim of this study was to evaluate the usefulness of  $^{18}\text{F}$ -fluorodeoxyglucose (FDG) positron emission tomography (PET)/computed tomography (CT) for the diagnosis of a portal vein tumor thrombus (PVTT) in patients with hepatocellular carcinoma (HCC).

**Methods** One hundred fifty-four patients with histologically proven HCC underwent  $^{18}\text{F}$ -FDG PET/CT imaging. The maximum standardized uptake value (SUVmax) was calculated, and the change in SUVmax (retention index, RI) was defined as the ratio of the increase in SUVmax between early and delayed scans to the SUVmax in the early scan. The circular region of interest was placed on the transaxial images according to the corresponding CT images. The final diagnoses of a PVTT were confirmed by histopathology.

**Results** Of the patients examined, 101 (65.6%) had no confirmed instances of a PVTT, whereas 53 (34.4%) had a confirmed PVTT. The sensitivity of  $^{18}\text{F}$ -FDG PET/CT imaging was 62.3%, the specificity was 97.0%, the accuracy was 85.1%, the positive predictive value was 91.7%, and the negative predictive value was 83.1%. The SUVmax of the PVTT was  $4.32 \pm 1.96$  and the SUVmax of the HCC lesions for these patients was  $5.38 \pm 2.79$ , but these differences were insignificant ( $t = 1.78$ ,  $p = 0.08$ ). For dual-time-point imaging, the SUV1 of the PVTT lesions was  $3.75 \pm 1.48$ , and SUV2 was  $3.63 \pm 1.41$ , but these differences were insignificant ( $t = 0.82$ ,  $p = 0.42$ ). The SUV1 of the HCC lesions was  $4.47 \pm 2.03$ , and the SUV2 was  $4.90 \pm 2.07$ , which were both also insignificant ( $t = -1.81$ ,  $p = 0.09$ ). The RI of the PVTT lesions was  $-2.05 \pm 19.96\%$ , and the RI of the HCC lesions was  $11.87 \pm 26.20\%$ , with no significant differences between them ( $t = 1.58$ ,  $p = 0.13$ ).

**Conclusions**  $^{18}\text{F}$ -FDG PET/CT may potentially improve the accurate diagnoses of a PVTT in patients with HCC.

**Keywords**  $^{18}\text{F}$ -FDG · PET/CT · Hepatocellular carcinoma · Portal vein tumor thrombus

## Introduction

Hepatocellular carcinoma (HCC) is one of the five most common cancers worldwide, with a particularly high prevalence in Asia due to endemic hepatitis B virus infection [1]. Although surgical resection or local ablative therapies achieve the best outcomes, with 5-year survival rates between 60 and 70% in patients treated during early stages of the disease, only about 30% are amenable to potentially curative treatment [2]. A portal vein tumor thrombosis (PVTT) is a common complication of HCC, which can lead to intrahepatic or distant metastases with poor prognosis. PVTTs are found in 10–40% of patients at diagnosis, and the median survival is only 2–4 months compared with 10–24 months in patients without a PVTT [3]. Although both computed tomography (CT) and magnetic resonance imaging (MRI) play important roles in the diagnosis of a PVTT, it is difficult

✉ Hongcheng Shi  
shihongcheng163@163.com

Bing Wu  
wbtank88@sina.com

Yiqiu Zhang  
zhang.yiqiu@zs-hospital.sh.cn

Hui Tan  
tan.hui@zs-hospital.sh.cn

<sup>1</sup> Department of Nuclear Medicine, Zhongshan Hospital, Fudan University, No. 180, Fenglin Road, Xuhui District, Shanghai, China

<sup>2</sup> Nuclear Medicine Institute of Fudan University, Shanghai, China

<sup>3</sup> Shanghai Institute of Medical Imaging, Shanghai, China

to identify whether the thrombus is malignant or benign. Positron emission tomography (PET)/CT using  $^{18}\text{F}$ -fluorodeoxyglucose ( $^{18}\text{F}$ -FDG) as a new diagnostic technique combining anatomic and metabolic information has been increasingly used for the detection and staging of a variety of malignant tumors. However, few studies have reported the use of  $^{18}\text{F}$ -FDG PET/CT in the detection of a PVTT in patients with HCC. The objective of this study was to retrospectively investigate the value of  $^{18}\text{F}$ -FDG PET/CT for the detection of a PVTT in patients with HCC.

## Materials and methods

### Patients

One hundred fifty-four patients, with suspected HCC, who underwent  $^{18}\text{F}$ -FDG PET/CT between June 2010 and December 2013 and received surgery (partial liver resection or liver transplantation) 4 weeks after the PET scan, were retrospectively reviewed. A diagnosis of HCC and a PVTT was based on histological proof. Informed consent was obtained from all patients participating in the study. Informed consent was waived because of the retrospective design of this study.

### PET imaging

PET studies were performed using a combined PET/CT scanner (Discovery VCT, GE Medical Systems, and Wisconsin-Milwaukee, USA). All patients were imaged after fasting for a minimum of 6 h with access to water and medications. Their blood sugar levels were measured prior to injection, and all levels were required to be less than 7 mol/L for patient inclusion.  $^{18}\text{F}$ -FDG was injected, intravenously, in activities of 5.1 MBq/kg (0.17 mCi/kg). Whole-body imaging was performed  $56.3 \pm 10.6$  min after  $^{18}\text{F}$ -FDG injection. The scans were performed while patients were in a supine position with arms over the head, and the scans were initiated with a diagnostic CT scan (200 mAs, 140 kV, 3.75 mm slice thickness) covering the thorax. These scans were used for attenuation correction and PET scans over the same region immediately followed (consisting of 6–7 bed positions for 2 min per table position). Delayed scans, which began approximately  $118.3 \pm 18.6$  min after  $^{18}\text{F}$ -FDG injection, acquired images from only the upper abdominal cavity where a malignancy was suspected from conventional imaging studies. PET image data were reconstructed, iteratively, using a row action, maximum likelihood algorithm, and segmented correction for attenuation with the use of the CT data (Matrix size  $512 \times 512$ , SFOV 50.0 cm, DFOV 50.0 cm, slice thickness 1.25 mm). Integrated, co-registered PET/CT images were obtained by means of a Xeleris workstation

(GE Medical Systems), which enabled image fusion and analysis. The images were reconstructed and displayed in three dimensions; axial, sagittal, and coronal reconstructions were subsequently used for interpretation.

### Imaging data analysis

Two experienced nuclear medicine physicians, unaware of the histological results, interpreted all PET/CT findings by consensus. Abnormal low-density lesions in the right branch, left branch, or main portal vein on the CT images had corresponding abnormal elevated glucose metabolism observed on the PET images. The circular region of interest (ROI) was placed on the transaxial images according to the corresponding CT images. The ROI was placed the same peripheral position of the liver in the first and delayed scans. The maximum standardized uptake value of each lesion was measured. Furthermore, for patients who had dual-time-point scans, we calculated the RI-SUVmax from the SUVmax according to the following formula:  $\text{RI-SUVmax (\%)} = [\text{SUV2 (delayed scan)} - \text{SUV1 (early scan)}] * 100 / \text{SUV1 (early scan)}$ . While the lesions cannot be seen in the non-enhanced CT, we will consult the enhanced CT or MRI within a month.

### Statistical analysis

Data were analyzed with the SPSS statistical package (SPSS Windows, version 19.0). Metrics such as age and maximum SUV of lesions were expressed using the mean  $\pm$  SD. Nominal data are presented by percentages. Furthermore, a 95% confidence interval for differences in paired proportions was calculated. A *p* value less than 0.05 was considered significant.

## Results

### Population

One hundred fifty-four patients, comprising 140 men and 14 women, with a mean age ( $\pm$  SD) of  $51.6 \pm 11.1$  years (range 16–80 years) at the time of diagnosis were included. Patient characteristics including age, sex, and histological grade are summarized in Tables 1 and 2.

### PET/CT imaging

Tables 3 and 4 show the diagnostic value of  $^{18}\text{F}$ -FDG PET/CT for a diagnosis of a PVTT. The sensitivity was 62.3%, the specificity was 97.0%, the accuracy was 85.1%, the positive predictive value was 91.7%, and the negative predictive value was 83.1%.

**Table 1** Patient characteristics

Characteristics	Number of patients (n = 154)
Age, years (mean ± SD)	51.1 ± 11.1
Sex, n (male/female)	140/14
Histological grade	
Grade I	7
Grade II	81
Grade III	65
Grade IV	1
PVTT–	101 (65.6%)
PVTT+	53 (34.4%)

**Table 2** Patients with PVTT

Characteristics	Number of patients (n = 53)
Position	
Right branch	23
Left branch	18
Main branch	7
Both left and main branches	1
All branches	4
Histological grade	
Grade II	21
Grade III	32

**Table 3** The diagnostic value of <sup>18</sup>F-FDG PET/CT for PVTT

Groups	PET/CT imaging (+)	PET/CT imaging (–)	Total
With PVTT	33	20	53
Without PVTT	3	98	101
	36	118	154

**Table 4** The histological grade of the results

	True-positive	False-positive	True-negative	False-negative
Grade I	–	–	7	–
Grade II	12	2	53	14
Grade III	20	1	38	6
Grade IV	–	–	1	–

The SUVmax of the PVTT was  $4.33 \pm 1.96$ , and the SUVmax of the HCC lesions for these patients was  $5.39 \pm 2.79$ , with no significant differences between them ( $t = 1.78$ ,  $p = 0.08$ ) (Figs. 1, 2). In all 154 patients, 129 patients underwent a dual-time-point PET/CT scan. Table 5 shows the SUVmax and diameter. Among the 33 patients with a PVTT, 14 patients underwent a dual-time-point PET/CT scan. Table 6 shows the SUVmax and RI-SUVmax values. The SUV2 of the PVTT was lower than SUV1, but there were no significant differences between them ( $t = 0.82$ ,  $p = 0.42$ ). Whereas the SUV2 of HCC was higher than SUV1, there were also no significant differences between them ( $t = -1.81$ ,  $p = 0.09$ ). Although the SUV1, SUV2, and RI of the HCC lesions were all higher than those of the PVTT lesions, there were still no significant differences between them (SUV1:  $t = 1.08$ ,  $p = 0.29$ ; SUV2:  $t = 1.90$ ,  $p = 0.07$ ; RI  $t = 1.58$ ,  $p = 0.13$ ). For the HCC lesions, only 4 (28.6%) patients had SUV2 values lower than the SUV1 values, and 8 (57.1%) patients had SUV2 values lower than the SUV1 values for PVTT lesions.

## Discussion

A diagnosis of HCC is often associated with poor prognosis, stemming from many factors, such as a PVTT [4]. The formation of a PVTT is associated with the anatomy, hemodynamics, and biology characteristic of the tumor. With the development of HCC, branches of the hepatic artery and portal vein open when the main vessels are blocked. Tumor cells along the hepatic artery can travel into the portal system and violate the vein wall to become a PVTT, which can lead to intrahepatic or distant metastases [5]. A diagnosis of a PVTT with HCC contraindicates using curative treatments. According to Milan criteria, liver transplantation is contraindicated in HCC patients with a PVTT. HCC patients with a PVTT are unable to benefit from local interventions, such as radiofrequency ablation, transcatheter arterial embolization, and percutaneous ethanol injection [6]. Takizawa et al. reported that in 193 HCC patients with a PVTT, the 1-, 2-, 3-, and 5-year survival rates were 37.5, 24.0, 18.9, and 8.3%, respectively [7]. An early diagnosis of a PVTT is very important to determine an appropriate clinical approach. Recently, <sup>18</sup>F-FDG PET/CT has been more widely used for the diagnosis of malignant tumors. Compared with CT and MRI, <sup>18</sup>F-FDG PET/CT has some advantages in the evaluation of HCC, including staging and restaging tumors, detection of recurrence and monitoring tumor response, but the accuracy of diagnosis is not satisfactory, especially for the well-differentiated HCC [8], and few studies have reported its application for the diagnosis of a PVTT [8–10].

<sup>18</sup>F-FDG PET/CT can provide both anatomical and metabolic information, and it is useful for both the diagnosis and

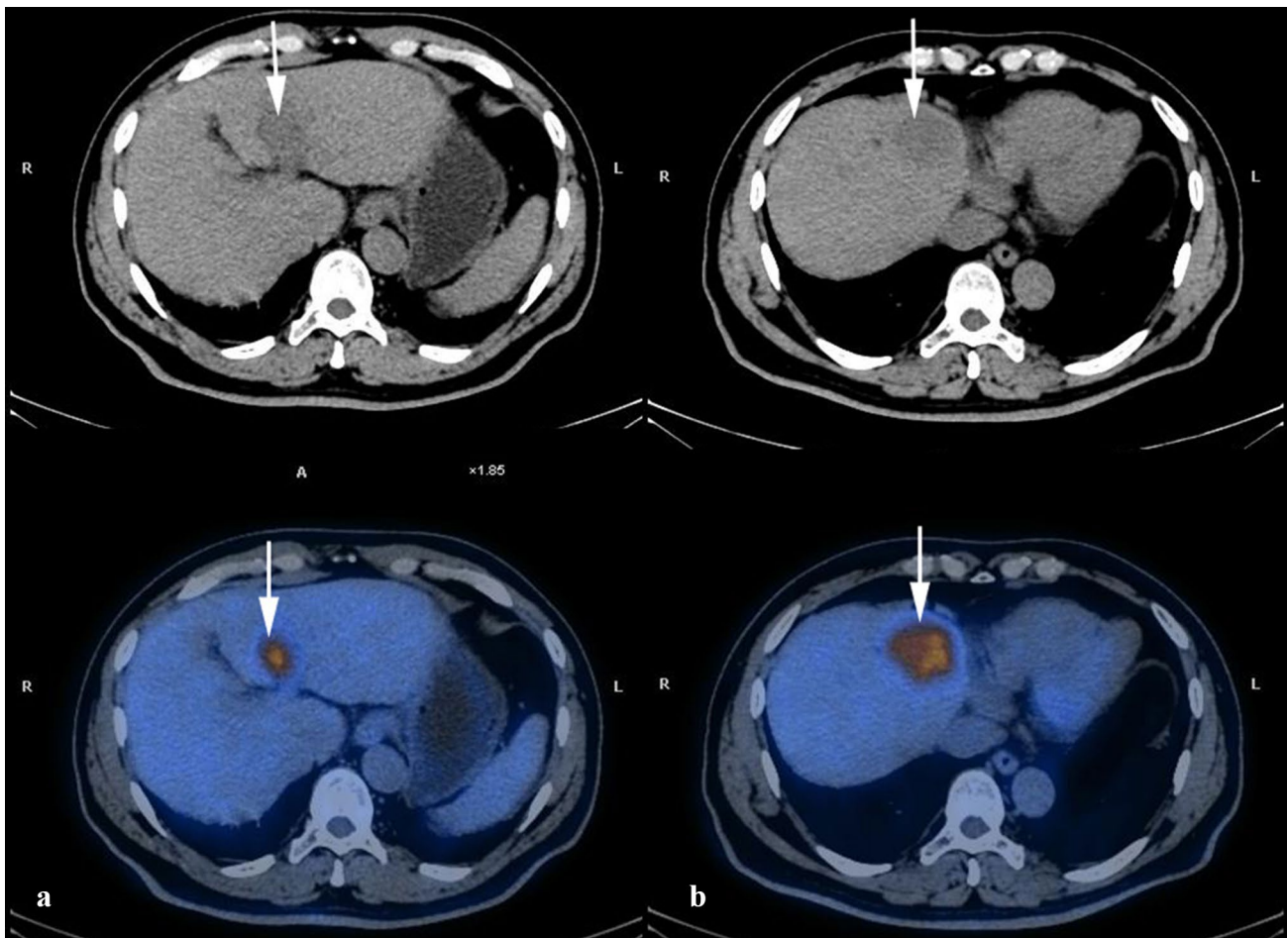


**Fig. 1 a** Male, 59 years. A non-contrast CT image shows a thrombus in the left portal vein. An integrated PET/CT image shows high FDG uptake (SUVmax=9.31) by the thrombus in the left portal vein. **b A**

non-contrast CT image shows a low-density lesion in the left lobe of the liver. The fused PET/CT image shows high FDG uptake (SUVmax=9.20) by the lesion. Pathological diagnosis was HCC, grade III

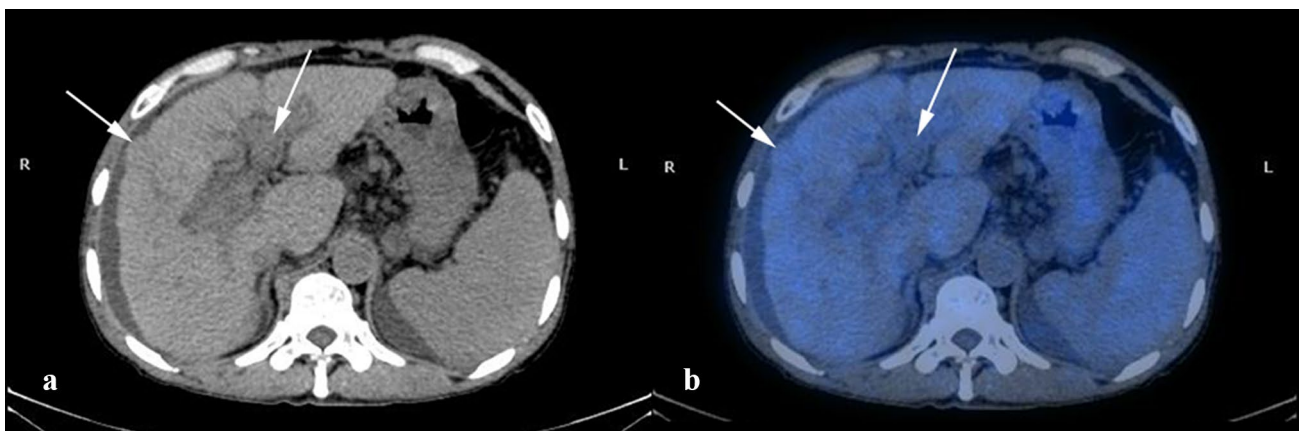


**Fig. 2 a** Male, 57 years. A non-contrast CT image shows a low-density nodule in the right lobe of the liver and the portal vein appears abnormally wide. **b A** fused PET/CT image shows no nodules in

the liver but a thrombus in the portal vein shows no abnormal FDG uptake. Pathological diagnosis was HCC, grade II, and the blood thrombus has necrotic tissues

**Table 5** SUVmax and diameter of HCC

	Grade I (n=4)	Grade II (n=69)	Grade III (n=55)	Grade IV (n=1)
SUV1	2.41 ± 0.33	3.57 ± 2.13	4.59 ± 3.19	5.4
SUV2	2.28 ± 0.46	3.87 ± 2.36	4.68 ± 3.55	11.1
Diameter (cm)	1.58 ± 0.33	3.59 ± 1.98	4.13 ± 3.56	6.67

**Table 6** SUVmax and RI-SUVmax

	HCC	PVTT	T test
SUV1	4.47 ± 2.03	3.75 ± 1.48	t = 1.08, p = 0.29
SUV2	4.90 ± 2.07	3.63 ± 1.41	t = 1.90, p = 0.07
T test	t = -1.81, p = 0.09	t = 0.82, p = 0.42	
RI (%)	11.87 ± 26.20	-2.05 ± 19.96	t = 1.58, p = 0.13

location of a tumor. During the process of tumor development, metabolic abnormalities tend to occur earlier than morphological abnormalities, which is why PET/CT can be used to locate the lesion before it appears morphologically abnormal. The primary modalities available to study PVTTs are ultrasound, CT, and MRI. Tarantino et al. reported that contrast-enhanced sonography had a sensitivity of 88% for diagnosing a PVTT compared with a sensitivity of 20% for color Doppler sonography [11]. Tublin et al. reported a sensitivity of only 43% and a specificity of 100% for an enhanced CT diagnosis of a PVTT [12]. Kumaresan et al. reported a sensitivity of 100% and a specificity of 90% for an enhanced MRI diagnosis of a PVTT, but the PVTT, in his study, was distant from the HCC lesion, which was greater than 5 cm in size. Several studies had reported the value of  $^{18}\text{F}$ -FDG PET/CT in the diagnosis of PVTT [13–15]. Hu et al. reported  $^{18}\text{F}$ -FDG PET/CT was a promising new method for distinguishing between portal venous neoplastic thrombosis and blood thrombosis with the optimal cut-off value of SUVmax > 3.35 as a criterion [15]. Sun et al., Hanajiri et al. and Beadsmooret et al. both reported cases, in which  $^{18}\text{F}$ -FDG PET/CT was more sensitive than conventional CT and MRI in detecting suspected PVTTs in patients with HCC [16–18].

Besides HCC, cirrhosis and portal hypertension can also cause thrombus. It is very important to differentiate a PVTT from a portal vein blood thrombus in the early stages of HCC. Traditionally, ultrasound, enhanced CT, and MRI are used to detect a PVTT, but it is difficult to identify whether the thrombus is malignant or benign. In our study, 53 patients were diagnosed with PVTT; the sensitivity of  $^{18}\text{F}$ -FDG PET/CT for the diagnosis was 62.3%, the specificity was 97.0%, the accuracy was 85.1%, the positive predictive value was 91.7%, and the negative predictive value was 83.1%. Additionally, three patients showed evidence of a portal vein blood thrombus in our study, which were all negative by PET imaging. Therefore,  $^{18}\text{F}$ -FDG PET/CT is

considered to be more accurate with a lower false-positive rate for diagnoses of PVTTs than traditional imaging methods. Furthermore, the 33 true-positive patients included 13 (39.4%) with grade II HCC and 20 (60.4%) with grade III HCC. The three false-positive patients included two (66.7%) with grade II HCC and one (33.3%) with grade III HCC, whereas the 20 false-negative patients included 14 (70%) with grade II HCC and 6 (30%) with grade III HCC. These results are consistent with the diagnosis use of  $^{18}\text{F}$ -FDG PET/CT in HCC with different pathology grades [7]. Some studies have reported that well-differentiated HCC often appears as a false-negative result on routine  $^{18}\text{F}$ -FDG PET images [19]. Thus, the use of  $^{18}\text{F}$ -FDG PET/CT can accurately diagnosis a PVTT in patients with high-grade HCC.

However, several reports have noted that dual-time-point PET/CT can improve the diagnoses of malignant tumors including HCC [20, 21]. Lin et al. reported that the SUVmax of HCC lesions increases over time. They also reported that the initial accuracy of 56.3% increased to 62.5% after 2 h [22]. Dirisamer et al. reported increased FDG uptake in hepatic metastatic lesions, with the SUVmax increasing from 6.59 on a 1-h image to 8.09 on a 2-h image [23]. In our study, the SUVmax of HCC lesions tended to increase over time, but this increase was not significant. In the presence of a PVTT, the SUVmax tended to decrease over time, but was not significant. Metabolic trapping through phosphorylation by hexokinase is the rate-limiting step for intracellular  $^{18}\text{F}$ -FDG retention. This process can be reversed by glucose-6-phosphatase. Interestingly, normal tissue cells contain high levels of glucose-6-phosphatase, whereas malignant tumor cells have low levels of this enzyme but high levels of hexokinase [24].

In conclusion, our study demonstrates that  $^{18}\text{F}$ -FDG PET/CT is highly accurate for the detection of PVTTs, especially in patients with high-grade HCC. However, the value of dual-time-point imaging for PVTT diagnoses needs further clinical studies with a larger number of subjects. As there are few reports on dual-time-point PET/CT for PVTT diagnoses, it is unclear why PVTTs have opposite features of HCC. A larger, more in-depth study is needed.

## Compliance with ethical standards

**Conflict of interest** The authors declare that they have no conflict of interest.

## References

- Parkin, D.M., et al., Estimating the world cancer burden: Globocan 2000. *Int J Cancer*, 2001. 94(2): p. 153-6.
- Ahn, S.J., et al., (1)(8)F-FDG PET metabolic parameters and MRI perfusion and diffusion parameters in hepatocellular carcinoma: a preliminary study. *PLoS One*, 2013. 8(8): p. e71571.
- Lau, W.Y., et al., Treatment for hepatocellular carcinoma with portal vein tumor thrombosis: the emerging role for radioembolization using yttrium-90. *Oncology*, 2013. 84(5): p. 311-8.
- Kim, J.M., et al., The effect of alkaline phosphatase and intrahepatic metastases in large hepatocellular carcinoma. *World J Surg Oncol*, 2013. 11: p. 40.
- Rogoveanu, I., et al., Diagnostic particularities in primitive diffuse form hepatocellular carcinoma associated with portal vein thrombosis. *Rom J Morphol Embryol*, 2005. 46(4): p. 317-21.
- Llovet, J.M., et al., Natural history of untreated nonsurgical hepatocellular carcinoma: rationale for the design and evaluation of therapeutic trials. *Hepatology*, 1999. 29(1): p. 62-7.
- Takizawa, D., et al., Hepatocellular carcinoma with portal vein tumor thrombosis: clinical characteristics, prognosis, and patient survival analysis. *Dig Dis Sci*, 2007. 52(11): p. 3290-5.
- Kurtovic, J., H. Van Der Wall and S.M. Riordan, FDG PET for discrimination between tumor extension and blood thrombus as a cause for portal vein thrombosis in hepatocellular carcinoma: important role in exclusion of transplant candidacy. *Clin Nucl Med*, 2005. 30(6): p. 408-10.
- Aras, M., et al., FDG PET/CT appearance of portal vein tumor thrombus in the gastric primitive neuroectodermal tumor: uncommon primary tumor site with rare finding. *Clin Nucl Med*, 2013. 38(1): p. 47-9.
- Sun, L., et al., Positron emission tomography/computed tomography with (18)F-fluorodeoxyglucose identifies tumor growth or thrombosis in the portal vein with hepatocellular carcinoma. *World J Gastroenterol*, 2007. 13(33): p. 4529-32.
- Tarantino, L., et al., Diagnosis of benign and malignant portal vein thrombosis in cirrhotic patients with hepatocellular carcinoma: color Doppler US, contrast-enhanced US, and fine-needle biopsy. *Abdom Imaging*, 2006. 31(5): p. 537-44.
- Tublin, M.E., G.R. Dodd and Baron RL, Benign and malignant portal vein thrombosis: differentiation by CT characteristics. *AJR Am J Roentgenol*, 1997. 168(3): p. 719-23.
- Erhamamci, S., et al., Incidental diagnosis of tumor thrombosis on FDG PET/CT imaging. *Rev Esp Med Nucl Imagen Mol*, 2015. 34(5): p. 287-94.
- Bagni, O., et al., (18)F-FDG PET/CT imaging of massive portal vein tumor thrombosis from ileal adenocarcinoma. *Hell J Nucl Med*, 2014. 17(1): p. 52-3.
- Hu, S., et al., The role of 18F-FDG PET/CT in differentiating malignant from benign portal vein thrombosis. *Abdom Imaging*, 2014. 39(6): p. 1221-7.
- Hanajiri, K., et al., 18F-FDG PET for hepatocellular carcinoma presenting with portal vein tumor thrombus. *J Gastroenterol*, 2005. 40(10): p. 1005-6.
- Beadsmoore, C.J., et al., Hepatocellular carcinoma tumour thrombus in a re-canalised para-umbilical vein: detection by 18-fluoro-2-deoxyglucose positron emission tomography imaging. *Br J Radiol*, 2005. 78(933): p. 841-4.
- Sun, L., et al., Highly metabolic thrombus of the portal vein: 18F fluorodeoxyglucose positron emission tomography/computer tomography demonstration and clinical significance in hepatocellular carcinoma. *World J Gastroenterol*, 2008. 14(8): p. 1212-7.
- Sacks, A., et al., Value of PET/CT in the management of primary hepatobiliary tumors, part 2. *AJR Am J Roentgenol*, 2011. 197(2): p. W260-5.
- Shum, W.Y., et al., Clinical usefulness of dual-time FDG PET-CT in assessment of esophageal squamous cell carcinoma. *Eur J Radiol*, 2012. 81(5): p. 1024-8.
- Fuster, D., et al., [Dual-time point images of the liver with (18)F-FDG PET/CT in suspected recurrence from colorectal cancer]. *Rev Esp Med Nucl Imagen Mol*, 2012. 31(3): p. 111-6.
- Lin, C.Y., et al., 18F-FDG PET or PET/CT for detecting extrahepatic metastases or recurrent hepatocellular carcinoma: a systematic review and meta-analysis. *Eur J Radiol*, 2012. 81(9): p. 2417-22.
- Dirisamer, A., et al., Dual-time-point FDG-PET/CT for the detection of hepatic metastases. *Mol Imaging Biol*, 2008. 10(6): p. 335-40.
- Tsuda, M., et al., Time-related changes of radiofrequency ablation lesion in the normal rabbit liver: findings of magnetic resonance imaging and histopathology. *Invest Radiol*, 2003. 38(8): p. 525-31.

**Publisher's Note** Springer Nature remains neutral with regard to jurisdictional claims in published maps and institutional affiliations.